UDC 629.7(045)
DOI: 10.15587/2706-5448.2025.339717

Daniil Marshalok,
Oleksandr Luppo

MODELING COMBINED AND SEPARATED SEQUENCING LEGS IN POINT MERGE: IMPACT ON CAPACITY, VERTICAL PROFILE, AND CONTINUOUS DESCENT

The object of research is the process of arrival sequencing in terminal maneuvering areas under the Point Merge concept. One problematic aspect is ensuring stable time-based intervals and maintaining continuous-descent profiles under peak demand and wind perturbations, as well as the lack of simple rules for choosing between combined and separated sequencing legs and for switching between them. The study used analytical modelling of arc geometry and direct-to-merge rules; parameterization of procedures and target intervals; probabilistic models of demand and ground-speed variation; Monte Carlo simulations using open traffic, weather and Aeronautical Information Services sources; statistical analysis; construction of a proxy controllability index; a hysteresis-based switching rule; and sensitivity analysis. It was proposed to obtain a reproducible framework for designing and comparing combined and separated sequencing legs with unified metrics. This follows from combining transparent geometry parameterization with a simple hysteresis-based switching rule that avoids frequent back-and-forth configuration changes. As a result, medians are practically identical on identical geometry, while differences appear in the tails: separated legs reduce the probability of long loops and extreme low-altitude horizontal segments. Compared with static alternatives, hysteresis-based switching under peak demand reduces separation-interval violations by up to ≈ 17.5 percentage points and shortens median low-altitude horizontal time by ≈ 4–9 s, at the cost of ≈ 0.57 NM of added median distance, providing better operational support without heavy optimizers. Limitations include a single case, environmental inference via extra distance, and a proxy controllability index. Future work will include human-in-the-loop experiments and coupling with detailed aircraft-performance models.

Keywords: *Point Merge, sequencing legs, continuous descent, capacity, separation interval.*

Received: 21.07.2025
Received in revised form: 20.09.2025
Accepted: 13.10.2025
Published: 30.10.2025

How to cite
Marshalok, D., Luppo, O. (2025). Modeling combined and separated sequencing legs in Point Merge: impact on capacity, vertical profile, and continuous descent. Technology Audit and Production Reserves, 5 (2 (85)), 65–70. https://doi.org/10.15587/2706-5448.2025.339717

1. Introduction

Terminal maneuvering areas are characterized by volatile demand, mixed fleets and strict environmental and noise constraints, which require arrival procedures to jointly ensure safety, throughput and reproducible descent profiles.

Solutions that reduce tactical vectoring, stabilize headways and ease controller workload while remaining compliant with regulatory requirements are of practical value.

The Point Merge concept organizes arrival flows on equal-distance arcs with direct-to-merge clearances, enabling controlled path stretching and predictable approach trajectories. Under peak loads or adverse winds, however, static layouts may exhibit tail risk behavior such as long loops or extended low-altitude level-offs, degrading environmental metrics and perceived workload. Transparent, reproducible rules for selecting the configuration and simple switching mechanisms between layout variants remain a relevant implementation need in real TMAs.

The regulatory framework delineates the design space for procedures: Procedures for Air Navigation Services – Air Traffic Management (PANS-ATM) sets principles of longitudinal separation and rules for their application to arrival-flow management [1]. Annex 11 defines the scope and objectives of Air Traffic Service (ATS), providing the service and organizational context in which sequencing procedures and phraseology are agreed [2]. EUROCONTROL's operational definition of Point Merge describes equal-distance arcs, direct-to-merge clearances and path-stretching mechanisms for harmonized queue control [3]. International Civil Aviation Organization's guidance on Continuous Descent Operations (CDO) links arrival-profile design to the minimization of low-altitude level-offs, noise and emissions, setting vertical-profile objectives for arrivals [4].

Early Point Merge studies reported reduced reliance on tactical heading vectoring and more repeatable trajectories relative to conventional radar vectoring [5]. EUROCONTROL's implementation guidance consolidates typical advantages and limitations of the concept, including effects on spacing regularity and controller workload, and outlines practical aspects of deployment [6]. Geometry-arc radius, entry-sector width, and merge-point placement shapes achievable headways and path-stretching options under varying demand [7]. Fast-time modelling of merging techniques shows that sequencing sensitivity to delay and variability depends on arc parameters and release rules from radius-to-fix segments [8].

Contemporary evaluations indicate that tuning Point Merge to local conditions can jointly reduce delays and the environmental footprint of arrivals [9]. Multi-arrival route designs demonstrate fuel-efficiency gains at the cost of trade-offs in spacing regularity and path length [10]. Parallel and multi-merge architectures increase scheduling complexity

ISSN-L 2664-9969; E-ISSN 2706-5448

and sensitivity to demand surges, calling for more sophisticated sequencing logic [11]. Methodologically, sequencing problems in ATS are multi-criteria under uncertainty, requiring a balance of safety proxies, efficiency, environmental impact, and human workload [12].

Despite substantial progress, the literature lacks integrated comparisons of combined versus separated sequencing legs on identical geometry and procedures.

With a focus on headway stability, low-altitude level-off time and controllability proxies. Simple, implementation-ready rules for dynamic switching between configurations-responsive to demand and ground-speed perturbations without heavy optimization are also insufficiently described.

The aim of the research is to develop a transparent, reproducible framework for designing and comparing combined and separated sequencing legs in Point Merge with unified metrics. And to formulate a hysteresis-based switching rule that preserves time-based separation and CDO conformance across demand regimes with minimal added track miles.

To achieve this aim, the following objectives are accomplished:

1. Build a reproducible Point Merge framework formalizes geometry and direct-to-merge procedures with explicit assumptions and constraints.
2. Design and validate a hysteresis-based switching policy between layouts, including anti-chatter thresholds for stable operation under fluctuating demand and wind. Quantify effects and sensitivities.
3. Derive operational guidance for local deployment, including calibration and applicability conditions.

2. Materials and Methods

The object of research is the process of arrival sequencing and integrated control in terminal maneuvering areas using the Point Merge concept. The focus is the design and comparative evaluation of combined and separated sequencing legs on identical procedures and geometry, together with a demand-aware switching rule between layouts. The study is therefore of a review and theoretical nature, based on open sources of technical, scientific, and applied literature. In the study, the following scientific methods were used. The method of analysis is to derive kinematic and procedural relations. The method of classification to distinguish layout variants and operating regimes. Analytical modelling to link geometry and time-based spacing. Geometric parameterization to define design variables and constraints. Probabilistic modelling to represent demand and wind-driven ground-speed variation. Monte-Carlo simulation to explore scenario spaces. Decision-rule design to trigger layout switching with hysteresis. Statistical analysis to summarize central tendency, dispersion, and tail risks. Sensitivity analysis to identify dominant factors. And operational proxy construction to approximate controller workload and controllability.

Analytical modelling links the arc geometry to time-based separation and feasibility. The relation between arc length, time delay, and ground speed defines how much controllable path-stretching is available on a given radius

$$\Delta s = R\Delta\theta, \tag{1}$$

where R – the arc radius (nautical miles (NM)), $\Delta\theta$ – the angular span (radians), Δs – the path length (NM)

$$\Delta t = \frac{\Delta s}{V_g}, \tag{2}$$

where Δt – the time in seconds, V_g – the ground speed along the arc.

The minimum angular spacing on the arc that guarantees the target headway at the merge follows directly from the kinematics

$$\Delta\theta_{\min} = \frac{\tau_{sep} V_g}{R_k}, \tag{3}$$

where τ – the target time-based separation (s), $\Delta\theta_{min}$ – the required angular spacing (radians).

Coordinated turn limits bound the minimum feasible radius for the planned speed and bank-angle constraint, which screens out non-implementable geometries before simulation

$$R_{\min} \approx \frac{V^2}{g\tan\varphi_{\max}}, \tag{4}$$

where V – the true airspeed, g – the gravitational acceleration, $\varphi_{\max}$ – the bank-angle limit.

Geometric parameterization defines two layouts on the same merge point and final approach. The combined layout uses a single equal-distance arc with a unified entry sector. The separated layout uses disjoint arcs or sectorized entries but keeps the same procedural parameters, including target separation, speed regimes, and direct-to-merge logic. Capacity at the merge is described in time units by the nominal headway target and in spatial terms by the number of aircraft simultaneously accommodated on the arc

$$\mu = \frac{3600}{\tau_{sep}} = \frac{60}{\tau_{sep}(\text{min})}\left[\frac{\text{flights}}{\text{hour}}\right], \tag{5}$$

where μ – the nominal merge throughput (flights per hour), τ – the target headway (s)

$$N_{\max} = \left\lfloor \frac{|\Theta_k|}{\Delta\theta_{\min}} \right\rfloor, \tag{6}$$

where N_{max} – the number of aircraft simultaneously on the arc, Θ_k – the usable arc span allocated to arrivals, $\Delta\theta_{min}$ – the minimum angular spacing.

The probabilistic model represents demand and wind as exogenous uncertainties. Arrival demand is stratified into low, medium, and peak regimes. Headway perturbations around the target emulate scheduling noise and operating variability. Ground-speed dispersion captures wind influence without prescribing a specific meteorological model. For reporting and reproducibility, arrival intensity is computed per minute and per hour from sliding five-minute counts:

$$\lambda_{per\,\min} = \frac{c_b}{5}, \tag{7}$$

$$\lambda_{perhour} = 60\lambda, \tag{8}$$

where λ – the arrival intensity, c_b – the count in the 5-minute window.

A discrete event Monte-Carlo engine propagates aircraft along arcs and merge legs under the defined procedures. Each simulation draws samples of a demand level and a set of wind-induced groundspeed realizations. The engine applies release rules and speed advisories and then evaluates the resulting headways at the merge. Scenario batches are sized to stabilize statistics. Random seeds are controlled to allow exact replication across compared layouts.

Performance metrics are harmonized across scenarios. Throughput is measured in flights per hour at the merge. Headway stability is summarized by the median, the interquartile range, and bootstrap-based 95% confidence intervals. Violation rate counts arrivals that fall below the target headway. Extra track miles provide a fuel and CO_2 proxy without requiring engine-specific models. Level-off time at low altitude quantifies vertical profile quality and CDO conformance. A controllability index aggregates counts of clearances and advisory changes with fixed weights to approximate controller workload

$$L = \alpha n_{instr} + \beta n\Delta V + \gamma n\Delta\psi, \quad (9)$$

where n_{instr} – the count of controller instructions, $n\Delta V$ speed changes, and $n\Delta\psi$ heading changes before direct-to-merge, and α, β, γ are weights.

The switching rule with hysteresis uses a sliding-window estimator of recent headway-target violations at the merge. The upper threshold triggers a switch to the more robust layout under stress. The lower threshold delays returning to the nominal layout, which prevents oscillations and nuisance switching. Window length and thresholds are chosen by sensitivity analysis rather than tuned to a single scenario.

Statistical treatment computes metrics per run and then aggregates them across runs within each regime. Medians, interquartile ranges, and confidence intervals are reported with identical random seeds for matched scenarios to reduce sampling variance. Tail risk is assessed with upper-percentile statistics and exceedance probabilities for long loops and extended level-offs. Implementation follows aviation units and conventions. Nautical miles are used for distance, and knots for speed. Seconds are used for time, and degrees for angles. All parameter files and seeds are archived for reproducibility.

Let's use two scenario sets: a daytime (calm) set representing ordinary intensity and a peak set with three demand levels defined by quantiles (Table 1). All analyses were conducted in Python within Visual Studio Code. METAR archives are used to classify calm (no significant wind) and crosswind conditions. Runway geometry and parameters are taken from electronic Aeronautical Information Publication and EAD. Data sources: OpenSky, AWC (NOAA/NWS), AIS/EAD [13–16].

Table 1

Demand levels by quantiles

Level	Quantile Q
Low	0.25
Medium	0.50
Peak	0.90

For parallel layouts and dynamic configuration changes, let's apply thresholds on a sliding separation violation rate with hysteresis to prevent frequent toggling under variable conditions [6, 10, 11].

3. Results and Discussion

Before moving to stochastic experiments, it is possible to verify that the kinematic and procedural relations behave as expected. For the chosen separated geometry, Table 2 fixes the key arc parameters and the nominal arc capacity used in the simulations.

This matches the usual rule of thumb: with a target separation of τ_{sep} = 120 s, the nominal throughput is about 30 flights per hour (Table 3), provided no tighter downstream constraints apply. Under both layouts, the delay absorbed on the arc is identical by construction: the median extra distance converts to median extra time

$$\Delta t_{med} \approx \Delta s / V_g,$$

consistent with (2) and the chosen arc geometry and speed.

Table 2

Key arc parameters and nominal capacity (separated geometry)

Flow	Arc radius (NM)	Angular span (deg)	Minimum angular spacing (deg)	Max a/c on arc	Target separation (s)	Mean ground speed (kt)	Nominal throughput (flights/h)
A	14	90	23.1911488505333	3	120	170	30.0
B	14	90		3	120	170	30.0

Table 3

Baseline metrics by configuration (deterministic check)

Configuration	Flow/aggregate	Extra distance, median (NM)	Max a/c on arc (count)	Throughput (flights/h)
Combined	A & B	5.667	3	30.00
Separated	A & B	5.667	3	30.00

For realistic conditions with fluctuating arrival demand, it is possible to construct samples of the arrival rate λ (flights/min) using 5-minute binning, define low/medium/peak levels by demand quantiles, and run Monte-Carlo simulations with fixed random seeds. Visually, the distributions of inter-aircraft spacing immediately before the merge are shown in Fig. 1: the bulk (body) of the distribution's overlaps, while the tails diverge, indicating where configuration effects are expected to emerge.

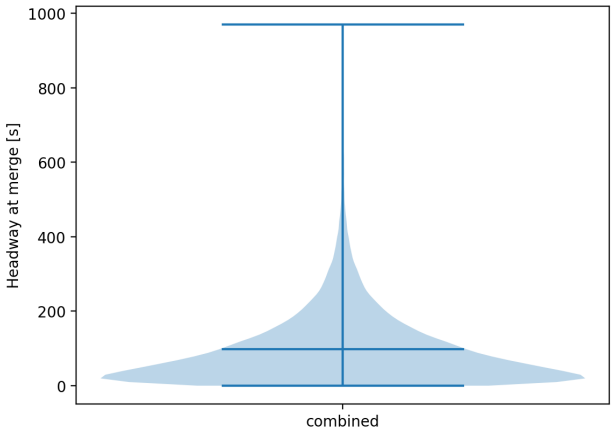

Fig. 1. Distributions of inter-aircraft spacing immediately before the merge

The share of violations of the target separation interval τ_{sep} by demand level is summarized in Table 4 and visualized in Fig. 2. The increase from "low" to "peak" is monotonic for both configurations, and the difference between the combined and separated layouts is small and falls within the 95% confidence intervals. Thus, a mere change of spatial organization does not by itself produce a large difference in violation rates-consistent with the data.

Table 4

Share of target separation interval violations by demand level

Configuration	Demand level	Throughput, μ (flights/h)	Violations of τ_{sep} (%)	95% CI: lower (%)	95% CI: upper (%)
Combined	low	30.00	33.33	11.76	51.72
Combined	medium	30.00	55.22	40.00	68.52
Combined	peak	30.00	70.04	58.73	78.57
Separated	low	30.00	33.16	12.50	51.52
Separated	medium	30.00	55.33	41.03	68.75
Separated	peak	30.00	70.04	58.06	79.31

Because CDO is a policy priority [4], it is also possible to examine level-off and the share of continuous descent approaches. Table 5 reports medians and quantiles of low-altitude level-off time. As demand rises, dispersion increases, while medians for the two configurations are close under low/medium demand. In peak conditions, an important nuance appears: upper quantiles are lower for the separated layout, i. e., there are fewer extreme level-offs.

ISSN-L 2664-9969; E-ISSN 2706-5448

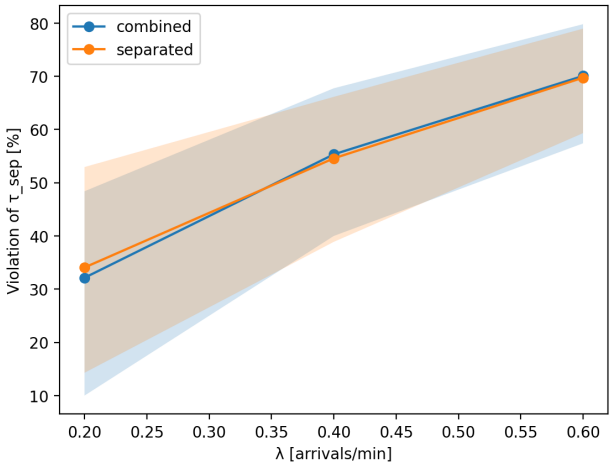

Fig. 2. Share of separation interval violations by demand level

Table 5

Low-altitude level-off time (median and quantiles)

Configuration	Scenario	Level-off time, median (s)	$Q_{0.1}$, s	$Q_{0.9}$, s
Combined	S1	25.1	3.3	92.6
Combined	S2	43.0	5.1	104.2
Combined	S3	60.9	7.7	110.4
Separated	S4	25.6	3.3	110.6
Separated	S5	47.7	5.2	124.0

From the standpoint of procedures and environmental impact, this is exactly the desired behavior: not the average but the tail regime drives noise, queue conflicts, and extra instructions. In other words, separated arcs act as a tail-control instrument, reducing the risk of very long horizontal segments. Environmental/fuel figures are kept at a proxy level: extra distance is converted to extra time via formula (2). Medians of extra distance are similar across configurations; the difference appears in the tails. On the cumulative curves (Fig. 3), the combined layout exhibits a longer right tail, whereas the separated layout reaches upper quantiles earlier. This indicates not about "average savings" as much as about reducing the probability of undesirable scenarios.

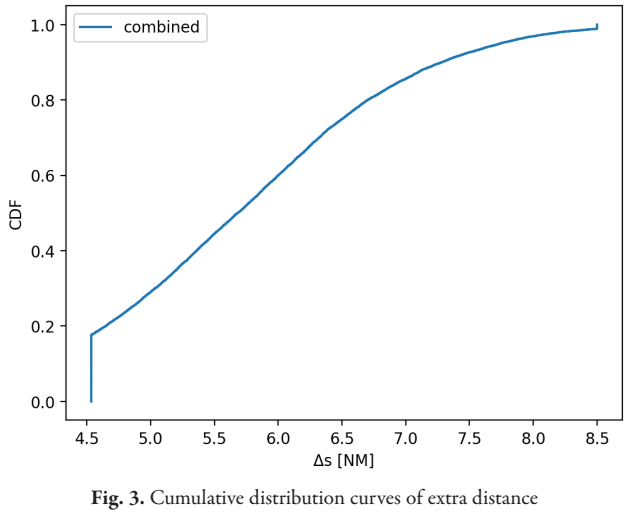

Fig. 3. Cumulative distribution curves of extra distance

It is possible to introduce a simple controllability index (formula (5)), which counts how many times the controller had to change heading, speed, and issue clearances up to the direct-to instruction. Under low and medium demand, the index L is lower for the combined layout: the more compact geometry implies fewer micro-corrections and a simpler crew mental model. At peak demand the difference fades: the binding constraint becomes the minimum angular spacing, and both configurations must maintain headways "at the limit". This profile aligns with EUROCONTROL practice notes on procedural acceptability and cognitive load [6, 12]. Table 6 summarizes the proxy controllability index L across scenarios and layouts, including component counts and the weights.

Table 6

Proxy controllability index

Configuration	Scenario	Controllability index L	Contribution			Weight (clearance, speed, heading)		
			clearances	speed changes	heading changes	α	β	γ
Combined	S1	0.724	0.537	0.137	0.050	1.0	0.7	0.5
Combined	S2	0.724	0.537	0.137	0.050	1.0	0.7	0.5
Combined	S3	0.808	0.621	0.137	0.050	1.0	0.7	0.5
Separated	S4	0.923	0.537	0.137	0.249	1.0	0.7	0.5
Separated	S5	0.923	0.537	0.137	0.249	1.0	0.7	0.5
Separated	S6	1.007	0.621	0.137	0.249	1.0	0.7	0.5

The most actionable result is the effect of controlled switching between layouts. When the sliding window share of τ_{sep} violations exceeds a threshold, the system switches from combined to separated; when the rate stabilizes, it switches back. In our data, under peak demand the violations reduce by up to ≈17.5 percentage points, the median extra distance increases only by ≈ 0.57 NM, and level-off time shortens (Table 7). In other words, at peaks it is possible to trade a small path "cost" for a substantial reduction in conflict potential and a cleaner vertical profile – a rational compromise consistent with PANS-ATM and CDO [1–4, 6, 10, 11].

Table 7

Effect of controlled switching

Metric	Before	After	Change	Scenario	Initial config
Violations of τ_{sep} (%)	33.33	25.00	−8.33	S1	Combined
Extra distance, median (NM)	5.670	6.237	+0.567	S1	Combined
Level-off time, median (s)	25.1	21.4	−3.8	S1	Combined
Violations of τ_{sep} (%)	55.22	41.42	−13.81	S2	Combined
Extra distance, median (NM)	5.664	6.231	+0.566	S2	Combined
Level-off time, median (s)	43.0	36.6	−6.5	S2	Combined
Violations of τ_{sep} (%)	70.04	52.53	−17.51	S3	Combined
Extra distance, median (NM)	5.668	6.235	+0.567	S3	Combined
Level-off time, median (s)	60.9	51.8	−9.1	S3	Combined
Violations of τ_{sep} (%)	33.16	33.16	0.00	S4	Separated
Extra distance, median (NM)	5.668	5.668	0.000	S4	Separated
Level-off time, median (s)	25.6	25.6	0.0	S4	Separated
Violations of τ_{sep} (%)	55.33	55.33	0.00	S5	Separated
Extra distance, median (NM)	5.666	5.666	0.000	S5	Separated
Level-off time, median (s)	47.7	47.7	0.0	S5	Separated
Violations of τ_{sep} (%)	70.04	70.04	0.00	S6	Separated
Extra distance, median (NM)	5.667	5.667	0.000	S6	Separated
Level-off time, median (s)	71.3	71.3	0.0	S6	Separated

With identical procedures and arc geometry, medians are nearly the same (Tables 3, 4). The hard boundary is the minimum angular spacing on the arc (2). If radius, angular span, target separation, and mean ground speed are equal, the safety threshold does not shift. Spatial organization mainly changes fluctuation structure and event dependence along the arc. Key differences appear in upper quantiles. Under peak demand, separated arcs reduce very long loops and shorten extra-miles tails, while medians remain close (Table 6, Fig. 3, Table 3). A similar pattern holds for the vertical profile. Median low-altitude level-off is similar, but upper quantiles are lower with separated geometry (Table 5). Nominal throughput set by the separation interval is about thirty flights per hour (Table 3). As demand rises to peak, violation shares increase monotonically for both layouts (Table 4, Fig. 2). These findings align with time-based separation and procedural logic, the review and analysis of which are performed in the source [1]. They fit the Point Merge path-stretching concept, the review and analysis concluded in [3]. They agree with early evidence on reduced tactical vectoring and repeatable paths, the review and analysis of which are performed in the source [5]. Geometry-driven effects match prior results, the review and analysis of which are performed in [7]. Environmental and delay benefits under tuned design are consistent with contemporary assessments, the review and analysis of which are done in [9]. For continuous descents, stability in busy hours matters more than mean level-off. Separated legs reduce very long level-offs in peak scenarios (Table 5). The controllability proxy indicates a more "obedient" combined layout at low and medium demand (Table 7). At peaks, this advantage disappears because separation and capacity dominate (2) and (5). Controlled switching with hysteresis is the main applied result. When the sliding-window violation share exceeds a threshold, switch to separated; return when the rate stabilizes. In peaks, switching reduces violations and shortens level-off time, with only a small rise in median extra miles (Table 7). Hysteresis prevents chattering and makes behavior predictable. Hence, based on the modeling, the following guidance proposed. It needs to adopt combined sequencing legs as the baseline under low–moderate demand, given their lower operational workload and comparable median performance. Under peak demand and during periods prioritizing continuous descent operations (CDO), prefer separated legs or implement a hysteresis-based switching policy between layouts. In all cases, calibrate arc radii, angular sectors, and time-based spacing to local airspace structure, noise constraints, fleet mix, and procedure design. All the settings must be validated through local performance assessment.

This research is limited to a single TMA geometry and a simplified environment: environmental impact is inferred from extra distance and controller workload is represented by a proxy index. Wind is modelled as ground-speed dispersion calibrated to representative METAR ranges, while surveillance and AMAN behaviors are idealized.

The results are reproducible. Using identical geometry and procedures, public parameter files, and fixed random seeds yields the reported medians, intervals, and tail metrics. To apply the method, calibrate target time-based separation, speed-advisory bounds, bank angle limit, wind dispersion ranges from METAR, and surveillance update rate to the local TMA. These results can be applied when arrivals use time-based spacing with direct-to-merge releases, speed advisories stay within the stated limits, and surveillance quality is comparable. Accordingly, outside these conditions, effects and thresholds may change. An exception concerns the exact flight-by-flight data for our sample days. Taken public source [13] limit historical retention, but it does not undermine reproducibility. The framework depends on calibrated distributions of demand and wind dispersion, plus fixed seeds, not on specific flight identities. Using a different but comparable period should give similar medians and 95% CIs. Only tail metrics may shift if the new period contains atypical weather or disruptions.

In the future work it is relevant to add human-in-the-loop trials, integrate performance-based fuel/CO_2 models and explicit wind fields, test multi-merge and multi-runway cases, and study data-driven switching thresholds.

4. Conclusions

1. A reproducible Point Merge framework that formalizes sequencing-arc geometry and direct-to-merge procedures under time-based spacing, bounded speed regimes, and standardized phraseology was developed. It was established that assumptions include time-based spacing, bounded speeds, and direct-to-merge releases, non-flyable geometries are excluded by these constraints and sector deconfliction rules. In order to benchmark the combined and separated layouts fairly, identical inputs and units are enforced. For comparison of the layouts across operating conditions, geometry and procedures are held constant while demand and wind are varied. The results show that separated legs reduce very long loops at peaks, but effects on extreme low-altitude level-off time are scenario-dependent.

2. In this study it was benchmarked switching vs static baselines using identical demand sequences and seeds. To determine the comparison the benefit of combined versus separated configurations, the same input realizations were used. Thus, through mathematical modeling, it has been shown that in peak scenarios, violations reduced by up to ≈ 17.5 percentage points, median level-off shortened by ≈ 4–9 s, and median extra distance rose only by ≈ 0.57 NM. This allows for the analysis of adaptive configuration management and stability under fluctuating load. Sensitivity highlights arc radius, entry-sector span, and merge-point placement as primary drivers, via their effect on $\Delta\theta_{\min}$ and $N_{\max}$.

3. These results have practical significance. Firstly, based on the modeling results, it was proposed actionable guidance for design and of continuous descent operations in TMA. Secondly, further research and applied developments can benefit from larger and richer datasets to strengthen external validity and automation, such as human-in-the-loop experiments that can quantify controller workload and confirm the proxy controllability index.

Conflict of interest

The authors declare that they have no conflict of interest in relation to this research, including financial, personal, authorship, or other interests, which could affect the research and its results presented in this article.

Financing

The research was conducted without financial support.

Data availability

The manuscript has associated data in a data repository.

Use of artificial intelligence

Computer-assisted text editing was used, namely during translation from Ukrainian to English; all methods, models, data, results, and conclusions are author's, with no automated generation of modeling outputs or empirical data.

References

1. *Procedures for Air Navigation Services – Air Traffic Management (PANS-ATM). Doc 4444* (2016) Montreal: ICAO. Available at: http://library.caanepal.gov.np:8080/bitstream/123456789/401/1/4444_cons_en.pdf

ISSN-L 2664-9969; E-ISSN 2706-5448

2. *Annex 11 to the Convention on International Civil Aviation: Air Traffic Services* (2018). Montreal: ICAO. Available at: https://ffac.ch/wp-content/uploads/2020/10/ICAO-Annex-11-Air-Traffic-Services.pdf
3. *Point Merge: Integration of arrival flows to a merge point. Operational Services and Environment Definition (OSED). Version 2.0* (2010). Brussels: EUROCONTROL. Available at: https://www.eurocontrol.int/sites/default/files/library/003_Point_Merge_OSED_V2.0.pdf
4. *Continuous Descent Operations (CDO) Manual. Doc 9931* (2010). Montreal: ICAO. Available at: https://applications.icao.int/tools/ATMiKIT/story_content/external_files/102600063919931_en.pdf
5. Favennec, B., Hoffman, E., Trzmiel, A., Vergne, F., Zeghal, K. (2009). The Point Merge Arrival Flow Integration Technique: Towards More Complex Environments and Advanced Continuous Descent. *9th AIAA Aviation Technology, Integration, and Operations Conference (ATIO).* https://doi.org/10.2514/6.2009-6921
6. *Point Merge implementation: A quick guide. Ed. 1.51* (2024). Brussels: EUROCONTROL. Available at: https://www.eurocontrol.int/sites/default/files/2024-12/eurocontrol-point-merge-guide-v1-51.pdf
7. Favennec, B., Trzmiel, A., Zeghal, K. (2018). How the geometry of arrival routes can influence sequencing? *2018 Aviation Technology, Integration, and Operations Conference.* https://doi.org/10.2514/6.2018-4000
8. Ivanescu, D., Shaw, C., Tamvaclis, C., Kettunen, T. (2009). Models of Air Traffic Merging Techniques: Evaluating Performance of Point Merge. *9th AIAA Aviation Technology, Integration, and Operations Conference (ATIO).* https://doi.org/10.2514/6.2009-7013
9. Hardell, H., Otero, E., Polishchuk, T., Smetanová, L. (2025). Optimizing air traffic management through point merge procedures: Minimizing delays and environmental impact in arrival operations. *Journal of Air Transport Management, 123,* 102706. https://doi.org/10.1016/j.jairtraman.2024.102706
10. Oren, A., Sahin, O. (2021). The flight efficiency analysis on the Multi-Arrival Route Point Merge System. *The Aeronautical Journal, 126 (1299),* 755–767. https://doi.org/10.1017/aer.2021.105
11. Dönmez, K., Çetek, C., Kaya, O. (2021). Aircraft Sequencing and Scheduling in Parallel-Point Merge Systems for Multiple Parallel Runways. *Transportation Research Record: Journal of the Transportation Research Board, 2676 (3),* 108–124. https://doi.org/10.1177/03611981211049410
12. Kharchenko, V. P., Butsyk, I. M., Alieksieiev, O. M. (2009). Methods of making the right decision Manager at Air Traffic Service. *Proceedings of National Aviation University, 40 (3).* https://doi.org/10.18372/2306-1472.40.1757
13. *OpenSky REST API.* OpenSky Network. Available at: https://openskynetwork.github.io/opensky-api/rest.html Last accessed: 07.10.2025
14. *Data API.* NWS Aviation Weather Center. Available at: https://aviationweather.gov/data/api/ Last accessed: 07.10.2025
15. *EIDW(DUBLIN) New Runway 10L/28R AIP IRELAND Updates* (2022). AirNav Ireland (AIS). Available at: https://www.iaa.ie/docs/default-source/publications/ei_sup_2022_020_en.pdf?sfvrsn=88d612f3_2
16. *European AIS Database.* EUROCONTROL. Available at: https://www.eurocontrol.int/service/european-ais-database Last accessed: 07.10.2025

✉***Daniil Marshalok,*** *PhD Student, Department of Air Navigation Systems, State University "Kyiv Aviation Institute", Kyiv, Ukraine, e-mail: 4646212@stud.kai.edu.ua, ORCID: https://orcid.org/0000-0001-5706-5794*

Oleksandr Luppo, *PhD, Associate Professor, Department of Air Navigation Systems, State University "Kyiv Aviation Institute", Kyiv, Ukraine, ORCID: https://orcid.org/0000-0001-9063-985X*

✉*Corresponding author*